

**Bending of pinned dust-ion acoustic solitary waves in presence of charged space debris**S. P. Acharya<sup>1,\*</sup>, A. Mukherjee<sup>2,†</sup> and M. S. Janaki<sup>1,‡</sup><sup>1</sup>*Saha Institute Of Nuclear Physics, AF Block, Sector-1, Salt Lake City, Kolkata, 700064, West Bengal, India*<sup>2</sup>*Physics and Applied Mathematics Unit, Indian Statistical Institute, Kolkata 700108, West Bengal, India*

(Received 3 January 2021; accepted 29 June 2021; published 26 July 2021)

We consider a low temperature plasma environment in the low Earth orbital region in the presence of charged space debris particles. The dynamics of (2+1)-dimensional nonlinear dust-ion acoustic waves with weak transverse perturbation, generated in the system, is found to be governed by a forced Kadomtsev-Petviashvili equation, where the forcing term depends on charged space debris function. The bending phenomena of some exact dust-ion acoustic solitary wave solutions in the  $x-t$  and  $x-y$  planes are shown; they result from the consideration of different types of possible localized debris functions. A family of exact pinned accelerated solitary wave solutions has been obtained where the velocity changes over time but the amplitude remains constant. The shape of the debris function also changes during its propagation. Also, a special exact solitary wave solution has been derived for the dust-ion acoustic wave that gets curved in spatial dimensions with the curvature depending upon the nature of the forcing debris function. Such intricate solitary wave solutions may be useful in modeling real experimental data.

DOI: [10.1103/PhysRevE.104.014214](https://doi.org/10.1103/PhysRevE.104.014214)**I. INTRODUCTION**

The upsurge in research on space plasma physics has achieved important results since the middle of the last century [1]. As a result, near-Earth space has become a virtual laboratory to study different physical properties of astronomical plasma system. In this context, the research on the dynamics of space debris objects has also increased drastically [2–4].

Space debris objects [2] include dead satellites, meteoroids, destroyed spacecraft, and other inactive materials resulting from many natural phenomena, which are being levitated in extraterrestrial regions, especially in near-Earth space. These space debris objects are substantially found in the low Earth orbital (LEO) and geosynchronous Earth orbital regions [3]. Also, their number is continuously increasing nowadays due to various artificial space missions which result in dead satellites, destroyed spacecraft, etc. The debris particles become charged in a plasma medium as the result of different mechanisms such as photoemission, electron and ion collection, secondary electron emission [5], etc. These charged debris particles of varying sizes (from as small as microns to as big as centimeters) [6,7] move with different velocities, causing significant harm to running spacecraft. Therefore, to avoid these deteriorating effects, active debris removal has become a challenging problem in the 21st century. Some indirect detection techniques for space debris objects have also been developed by different authors [4,7,8]. A new detection technique for charged debris objects in the LEO region was proposed by Sen *et al.* [7], making use of the interaction of nonlinear plasma waves with charged space debris. They considered the dynamics of nonlinear ion acoustic waves in (1+1)

dimensions and derived a forced Korteweg–de Vries (KdV) equation in which the forcing term depends on the debris function. Considering a Gaussian debris function, they predicted “precursor solitons,” which are emitted periodically, through numerical computation. Such precursors can be detected by appropriate sensors to give indirect evidence of the existence of charged space debris objects. Numerical techniques [9] have confirmed the existence of the pinned and precursor solitons even in the large amplitude generalization of the problem. Molecular dynamic simulations for a charged object moving at supersonic speed in a strongly coupled dusty plasma have also shown [10] the existence of precursor solitonic pulses and dispersive shock waves. Experimental investigations [11] carried out with dusty plasmas have corroborated the numerical findings and also observed [12] modifications in the propagation characteristics of precursor solitons due to the different shapes and sizes of the object over which the dust fluid flows.

In the ionospheric plasma region, the presence of dust particles with different charges and polarities cannot be ignored. These dust particles are weakly coupled, as in most space and astrophysical dusty plasmas. Shukla and Silint [13] first theoretically investigated the existence of low frequency dust-ion acoustic waves in plasmas. The presence of static charged dust particles in a plasma significantly affects the physical properties of dust-ion acoustic waves (DIAWs). Numerous theoretical works [14–30] have reported on studies of linear low frequency modes as well as the associated nonlinear coherent structures such as solitons, shocks, and vortices in different conditions for space and laboratory dusty plasmas. The excitation of linear and nonlinear perturbations in the upstream and downstream regions due to a charged moving object in such dusty plasmas has many practical implications in the context of space debris detection that deserve detailed investigation. Generally, subcentimeter sized debris particles in the ionospheric plasma are currently undetectable

\*siba.acharya@saha.ac.in; siba.acharya39@gmail.com

†abhikmukherjeesinp15@gmail.com

‡ms.janaki@saha.ac.in

through optical means [7,31]. The investigation of nonlinear ion acoustic waves in the presence of charged debris by different authors [7,31–33] has primarily intended to detect these subcentimeter sized debris particles. As discussed earlier, there are computational and experimental works [10–12] on dusty plasmas that considered moving charged objects and reported the observation of wakes and precursor solitons. These observations have been shown to be consistent with theoretical predictions based on the forced KdV equation that has been derived for a charged object moving in a plasma medium.

The forcing debris function mainly depends upon the size, shape, velocity, surface potential of the debris, Debye shielding effects, and distance of the point of observation from the debris [31,34]. The mathematical form of this debris function was derived by Truitt and Hartzell [31] in the form of a Gaussian function. Many authors have chosen various kinds of forcing functions like the  $\text{sech}^2$  and  $\text{sech}^4$  forms [7] or sinusoidal forms [35–37] to obtain solutions of the forced KdV equation. The chaotic dynamics of a nonlinear ion acoustic wave in the presence of the sinusoidal source debris term in Thomas-Fermi plasmas has also been explored [38].

In a real space plasma environment, it can be expected that both the amplitude and the velocity of the debris function may vary with time. In [33], a special ion acoustic solitary wave solution was derived in (1+1) dimensions for a specific pinned debris function where the velocity varies with time. Further, Sen *et al.* [7] showed that the  $\text{sech}^2$  form of the debris function leads to exact solutions of the forced KdV equation. The choice of a forcing term with arbitrary free functions allows the freedom to design more interesting solutions that may bend, twist, or turn during propagation. It is possible to find certain forms of debris functions for which exact solitary wave solutions can be obtained that have the bending features. On the other hand, the varying velocity of the debris function turns out to be identical to that of the solitary wave solutions; hence, they are pinned to each other, so accelerate or decelerate together. In the present work, some special exact (2+1)-dimensional solitary wave solutions for the dust-ion acoustic wave have been derived with both accelerating and bending features. An interesting intricate exact solution of the system is important for both experimental observations and validation of numerical simulations.

This paper is organized in the following manner. A detailed derivation of the (2+1)-dimensional nonlinear evolution equation for the dust-ion acoustic wave in the presence of a charged debris object is given in Sec. II. The exact accelerated pinned solitary wave solutions are derived in Sec. III. The exact curved solitary wave solution that can bend in the  $x$ - $y$  plane depending on the nature of the debris function is discussed in Sec. IV. In Sec. V, we discuss some dynamical and physical properties of the obtained solutions. Concluding remarks are given in Sec. VI.

## II. DERIVATION OF THE (2+1)-DIMENSIONAL NONLINEAR EVOLUTION EQUATION FOR THE DUST-ION ACOUSTIC WAVES IN THE PRESENCE OF CHARGED SPACE DEBRIS

We consider the low temperature plasma system in the LEO region in the presence of charged space debris particles.

Our aim is to find the evolution equation for the propagating finite amplitude nonlinear DIAWs generated in the system. As an extension of our previous problem on ion acoustic waves [33], we consider two-dimensional effects in the propagation of nonlinear dust-ion acoustic waves. The LEO region which we consider consists of a low density plasma along with an abundance of debris particles. The ion species is treated as a cold species; that is, ion pressure is neglected, and electrons obey the Boltzmann distribution. We neglect the dynamics of heavy and slow dust particles compared to the dynamics of the other particles present in the system. Hence, only the equilibrium dust density (independent of time) enters into the calculation through the charge neutrality condition. Following [39–41], the basic normalized nonlinear system of equations of our system in (2+1) dimensions is given by

$$\frac{\partial n}{\partial t} + \frac{\partial}{\partial x}(nu) + \frac{\partial}{\partial y}(nv) = 0, \quad (1)$$

$$\frac{\partial u}{\partial t} + u \frac{\partial u}{\partial x} + v \frac{\partial u}{\partial y} + \frac{\partial \phi}{\partial x} = 0, \quad (2)$$

$$\frac{\partial v}{\partial t} + u \frac{\partial v}{\partial x} + v \frac{\partial v}{\partial y} + \frac{\partial \phi}{\partial y} = 0, \quad (3)$$

$$\frac{\partial^2 \phi}{\partial x^2} + \frac{\partial^2 \phi}{\partial y^2} + n - (1 - \alpha)e^\phi - \alpha n_d = S(x, y, t), \quad (4)$$

where the following normalizations have been used:

$$\begin{aligned} x &\longrightarrow x/\lambda_d, & y &\longrightarrow y/\lambda_d, & t &\longrightarrow \frac{C_s}{\lambda_d} t, & n &\longrightarrow \frac{n}{n_{i0}}, \\ u &\longrightarrow \frac{u}{C_s}, & v &\longrightarrow \frac{v}{C_s}, & \phi &\longrightarrow \frac{e\phi}{k_B T_e}, \end{aligned} \quad (5)$$

where  $\lambda_d$  is the electron Debye length,  $C_s = \sqrt{\frac{k_B T_e}{m_i}}$  is the ion acoustic speed,  $k_B$  is Boltzmann's constant,  $T_e$  is the electron temperature,  $m_i$  is the ion mass, and  $n_{i0}$  is the equilibrium ion density. Equations (1)–(4) represent the ion continuity equation, ion momentum conservation equations in the  $x$  and  $y$  directions, and Poisson's equation, respectively, where  $n$ ,  $u$ ,  $v$ , and  $\phi$  denote the ion density,  $x$  and  $y$  components of the ion fluid velocity, and electrostatic potential, respectively. The parameter  $\alpha$  on the left-hand side of Poisson's equation (4) is given by

$$\alpha = Z_d \frac{n_{d0}}{n_{i0}}, \quad (6)$$

where  $Z_d$  and  $n_{d0}$  represent dust charge and equilibrium dust density, respectively.

The term  $S(x, y, t)$  on the right-hand side of Eq. (4) represents a charge density source arising due to a time varying debris object having two-dimensional space dependence, which creates a perturbation in the electric potential and density of the surrounding plasma. As a result, the plasma potential becomes modified due to the debris surface potential, which is discussed in detail in the work of Truitt and Hartzell for one dimension [31,34] and for two dimensions [32]. In their work, Truitt and Hartzell described this forcing or source debris function  $S(x, y, t)$  as Gaussian in nature in both one and two dimensions using the work of Grimshaw *et al.* [42]. The amplitude of this force debris function is given by the normalized plasma potential. Sen *et al.* [7] considered

localized solitary wave forms and the Gaussian form for the debris function. Taking these developments into account, we approximate the source debris function as

$$S(x, y, t) = \phi_{pm} S_d(x, y, t), \tag{7}$$

where  $\phi_{pm}$  denotes the normalized plasma potential and  $S_d(x, y, t)$  represents possible localized debris functions such as Gaussian, solitary wave types, etc., that move with velocities consistent with the debris object. In the work done by Sen *et al.* [7], ion acoustic solitary wave solutions for two specific forms of localized forcing debris functions were derived that also have the nature of solitary waves. The line solitary wave solutions have constant amplitudes and velocities, which was generalized in [33] by considering more realistic time dependent velocity for both the ion acoustic solitary wave and the forcing term.

The evolution equation corresponding to the nonlinear (2+1)-dimensional DIAWs is derived following the well-known reductive perturbation technique [43], where the dependent variables of the system are expanded as

$$n = 1 + \epsilon^2 n_1 + \epsilon^4 n_2 + O(\epsilon^6), \tag{8}$$

$$u = \epsilon^2 u_1 + \epsilon^4 u_2 + O(\epsilon^6), \tag{9}$$

$$v = \epsilon^3 v_1 + \epsilon^5 v_2 + O(\epsilon^7), \tag{10}$$

$$\phi = \epsilon^2 \phi_1 + \epsilon^4 \phi_2 + O(\epsilon^6), \tag{11}$$

where  $\epsilon$  is a small, dimensionless expansion parameter characterizing the strength of nonlinearity in the system. We consider a weak, space-time dependent localized debris function which vanishes at infinity. After scaling we have

$$S(x, y, t) = \epsilon^4 f(x, y, t), \tag{12}$$

where  $f(x, y, t)$  can have any spatially localized form that is consistent with the weakly coupled charged debris dynamics in the LEO region. The stretched coordinates are introduced as

$$\xi = \epsilon(x - v_p t), \quad \tau = \epsilon^3 t, \quad \eta = \epsilon^2 y, \tag{13}$$

where  $v_p$  is the phase velocity of the wave in the  $x$  direction. Accordingly, the differential operators are expressed in terms of the stretched variables as

$$\frac{\partial}{\partial x} = \epsilon \frac{\partial}{\partial \xi}, \quad \frac{\partial}{\partial t} = -\epsilon v_p \frac{\partial}{\partial \xi} + \epsilon^3 \frac{\partial}{\partial \tau}, \quad \frac{\partial}{\partial y} = \epsilon^2 \frac{\partial}{\partial \eta}. \tag{14}$$

Putting these expanded and rescaled variables in Eq. (1) and collecting different powers of  $\epsilon$ , we get

$$O(\epsilon^3) : -v_p \frac{\partial n_1}{\partial \xi} + \frac{\partial u_1}{\partial \xi} = 0, \tag{15}$$

$$O(\epsilon^5) : -v_p \frac{\partial n_2}{\partial \xi} + \frac{\partial n_1}{\partial \tau} + \frac{\partial}{\partial \xi} (u_2 + n_1 u_1) + \frac{\partial v_1}{\partial \eta} = 0. \tag{16}$$

Similarly, using Eq. (2), we get

$$O(\epsilon^3) : -v_p \frac{\partial u_1}{\partial \xi} + \frac{\partial \phi_1}{\partial \xi} = 0, \tag{17}$$

$$O(\epsilon^5) : -v_p \frac{\partial u_2}{\partial \xi} + \frac{\partial u_1}{\partial \tau} + u_1 \frac{\partial u_1}{\partial \xi} + \frac{\partial \phi_2}{\partial \xi} = 0. \tag{18}$$

Again, using Eq. (3), we get

$$O(\epsilon^4) : -v_p \frac{\partial v_1}{\partial \xi} + \frac{\partial \phi_1}{\partial \eta} = 0. \tag{19}$$

Finally, Eq. (4) yields

$$O(\epsilon^2) : -(1 - \alpha)\phi_1 + n_1 = 0, \tag{20}$$

$$O(\epsilon^4) : \frac{\partial^2 \phi_1}{\partial \xi^2} - (1 - \alpha)\phi_2 - (1 - \alpha)\frac{\phi_1^2}{2} + n_2 = f. \tag{21}$$

Now Eqs. (15), (17), (19), and (20) give

$$v_p n_1 = u_1, \quad v_p u_1 = \phi_1, \quad v_p^2 (1 - \alpha) = 1, \quad \frac{\partial v_1}{\partial \xi} = \frac{1}{v_p} \frac{\partial \phi_1}{\partial \eta}. \tag{22}$$

Hence, the phase velocity  $v_p$  is evaluated as

$$v_p = \pm \frac{1}{\sqrt{1 - \alpha}}, \tag{23}$$

where  $\alpha$  is defined in (6) and we consider the propagation along the positive  $x$  axis by choosing the positive sign for  $v_p$  in (23). From Eqs. (16) and (18), we get

$$\frac{\partial n_2}{\partial \xi} = \frac{1}{v_p} \left[ \frac{\partial n_1}{\partial \tau} + \frac{\partial (u_2 + n_1 u_1)}{\partial \xi} + \frac{\partial v_1}{\partial \eta} \right], \tag{24}$$

$$\frac{\partial u_2}{\partial \xi} = \frac{1}{v_p} \left[ \frac{\partial u_1}{\partial \tau} + u_1 \frac{\partial u_1}{\partial \xi} + \frac{\partial \phi_2}{\partial \xi} \right]. \tag{25}$$

The relations given by Eqs. (22), (24), and (25), after some simplification, give the following nonlinear evolution equation:

$$[n_{1\tau} + A n_1 n_{1\xi} + B n_{1\xi\xi\xi}]_{\xi} + C n_{1\eta\eta} = D f_{\xi\xi}, \tag{26}$$

where the subscript variables denote partial derivatives. The coefficients appearing in (26) are given as

$$A = \frac{v_p(3 - v_p^2)}{2}, \quad B = \frac{v_p^3}{2}, \quad C = \frac{v_p}{2}, \quad D = \frac{v_p}{2}. \tag{27}$$

This is the forced Kadomtsev-Petviashvili (KP) equation, i.e., the generalization of the nonlinear KdV equation to two-dimensional space. This is the final nonlinear evolution equation of the (2+1)-dimensional nonlinear DIAWs in the presence of charged space debris. Since we have assumed  $v_p$  is positive, Eq. (26) represents the forced KP-II equation. We normalize Eq. (26) to

$$[U_T + 6UU_X + U_{XXX}]_X + U_{YY} = F_{XX}, \tag{28}$$

where the new variables in (28) are defined as  $U = (\frac{A}{6B})n_1$ ,  $\xi = X$ ,  $T = B\tau$ ,  $Y = \sqrt{\frac{B}{C}}\eta$ ,  $F = (\frac{DA}{6B^2})f$ . Thus, we can see that the solutions of the forced KP-II equation (26) depend on the equilibrium dust parameters, i.e., on the parameter  $\alpha$  as well as on the charged space debris function  $f$ . In the following sections, we will find various exact solitary wave solutions of (26) with the special bending feature. Those solitary waves can bend on the  $x-t$  or  $x-y$  plane depending on the functional forms of the charged debris function  $f$ . The variations of the solitary wave solutions with the dust parameters will also be discussed. For mathematical simplicity, we will concentrate on the normalized equation (28) for further consideration. Finally, we can transform the solutions to the old variables to explore the physical picture.

### III. EXACT PINNED ACCELERATED SOLITARY WAVE SOLUTIONS

We have derived the forced KP-II equation (28) as the evolution equation for the nonlinear dust-ion acoustic wave in the presence of charged space debris particles. We know that Eq. (28) is, in general, nonintegrable and not exactly solvable. But if the forcing term obeys a definite constraint condition, the evolution equation can retain its integrability. This theory of converting a forced system into an integrable system is called the nonholonomic deformation theory, which is discussed in detail in [44,45]. Using this theory, we can show that Eq. (28) admits a special exact accelerated soliton solution under a specific integrable condition. The velocity of the soliton varies with time, whereas the amplitude remains constant. In this work, we will not go into the details of the integrability of the forced KP-II equation (28) by nonholonomic deformation theory [44,45]. Rather, we will concentrate on the exact solvability of Eq. (28). Sen *et al.* [7] derived two exact line solitary wave solutions for their forced KdV equation in (1+1) dimensions that have constant amplitude and velocity for the choice of two specific localized debris functions of  $\text{sech}^2$  and  $\text{sech}^4$  types.

In [32], the (2+1)-dimensional charged space debris function was derived as

$$F(X, Y, T) = N(\phi_s, r, \lambda_D) \exp \left\{ -\lambda_D^2 \left[ \left( \frac{X - V_X T}{R_X} \right)^2 + \left( \frac{Y - V_Y T}{R_Y} \right)^2 \right] \right\}, \quad (29)$$

where  $\phi_s$  denotes the surface potential of charged debris,  $r$  is the distance of the point of observation from the debris,  $\lambda_D$  represents the Debye length,  $V_X$  and  $V_Y$  represent the speeds of debris in the  $X$  and  $Y$  directions, respectively, and  $R_X$  and  $R_Y$  represent the radii of debris in the  $X$  and  $Y$  directions, respectively. In a realistic environment, the debris object may not have a perfectly spherical shape. A more complete and realistic picture of a debris object can be realized from a three-dimensional Gaussian function in an analogous manner. This can be referred to as the three-dimensional interpretation of debris and can be utilized to study the evolution of dust-ion acoustic waves in (3+1) dimensions. The amplitude of the forcing debris function  $F$  given by Eq. (29) depends on the surface potential of the debris object, the Debye length in the surrounding plasma medium, and the distance of the point of observation from the debris. The argument of the exponential function in Eq. (29) contains the space-time coordinates along with other constants. A few studies have been done in (1+1) dimensions by considering periodic forms of the debris function [35–37]. But several other types of localized functions can be chosen as forcing debris functions, which need not be exactly Gaussian but can represent similar behavior. In an actual disturbed situation in the LEO plasma region, there may be possibilities where the velocity of the debris may vary with time. Consequently, the expression for the forcing debris function gets modified in order to incorporate time varying velocity, which is also evident from Eq. (29). Several analytical forms of these kinds of time varying debris functions and the corresponding nonlinear dust-ion acoustic

waves can be explored to study many interesting phenomena. The mathematical forms of the two localized debris functions that were chosen for the derivation of the two exact pinned solitary wave solutions in [7] have a definite feature. It can be noticed that those debris functions are just constant multiples of the ion acoustic wave and its square. The solutions are mathematically interesting due to their pinned and exact nature. Motivated by this choice, we attempt to derive some special exact pinned solitary wave solutions for the dust-ion acoustic wave, the velocity of which varies with time depending on the specific debris function. Also, the acceleration associated with the solitary wave is expressed in terms of an arbitrary function that can be chosen appropriately to model the real physical phenomena. As stated in [31], pinned solitons are produced in the low LEO region, traveling at the same speed as the orbital debris. Since the pinned solitons propagate with the debris, they are not useful for on-orbit detection techniques as they would not be sensed before collision. However, pinned solitons can be detected from the ground sensors using the same techniques used to measure plasma density irregularities. The amplitudes of the solitary wave solutions which are discussed in this section are constant, whereas those of the debris function are variable. Such features may give rise to new directions in the detection process. We know that the  $\text{sech}^2$  function looks very similar to the Gaussian function. Hence, a forcing debris function that is estimated to have a Gaussian shape [32] can be chosen in the form of a  $\text{sech}^2$  function, and the understanding can also be generalized to higher dimensions. This type of forcing debris function is also a two-dimensional extension of the forcing debris functions chosen in the work of Sen *et al.* [7].

For the choice of the forcing debris function

$$F(X, Y, T) = a(T) U_m \text{sech}^2 \times \left[ \left( X + \int a(T) dT - d_1 T + Y \right) / w \right], \quad (30)$$

where  $U_m = \frac{(d_1-1)}{2}$ ,  $w = [2/\sqrt{(d_1-1)}]$ , with  $d_1$  being constant, and  $a(T)$  is an arbitrary function of time, an exact pinned solitary wave solution of Eq. (28) can be obtained as

$$U = U_m \text{sech}^2 \left[ \left( X + \int a(T) dT - d_1 T + Y \right) / w \right]. \quad (31)$$

A comparison of Eqs. (29) and (30) helps us identify various physical characteristics, i.e., size, shape, velocity, and surface potential, of realistic charged debris objects in the ionosphere. The velocity of the dust-ion acoustic solitary wave solution (31) changes over time, showing accelerating or decelerating features due to the presence of the function  $a(T)$  in its argument, whereas its amplitude remains constant. Both the amplitude and velocity of the source debris function  $F$  (30) change over time, showing shape changing effects. Since the analytic forms of the time varying velocities of both  $U$  and  $F$  are identical, they move together. So they can also be regarded as “pinned accelerated solitary waves,” as discussed in [7].

The pinned nature of  $U$  and  $F$  can be seen from Fig. 1 for a given choice:  $a(T) = -5e^{-(2T)}$ , where the dynamical evolution of both  $U$  and  $F$  is shown by plotting the functions at different times. The three-dimensional (3D) plots of

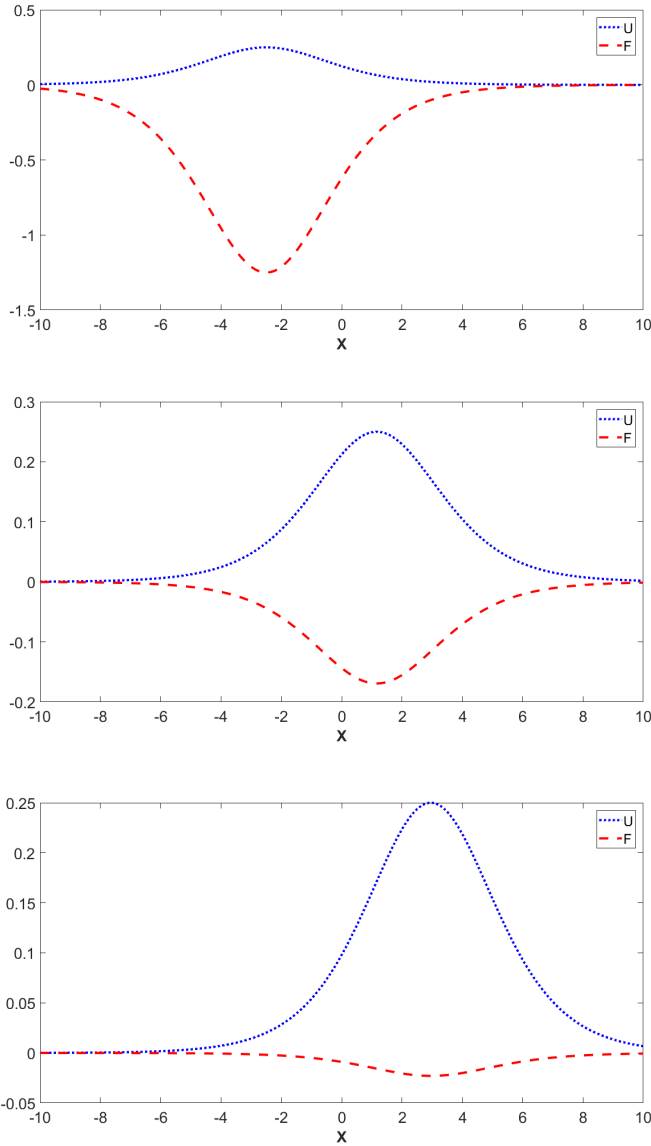


FIG. 1. Plots of the decelerated solitary wave solution  $U$  given by Eq. (31) and the forcing function  $F$  given by Eq. (30) with  $X$  at  $Y = 0$  for times  $T = 0, T = 1$ , and  $T = 2$  for the choice of  $d_1 = 1.5$  and  $a(T) = -5e^{-2T}$ . The top, middle, and bottom panels indicate the natures of  $U$  and  $F$  at  $T = 0, T = 1$ , and  $T = 2$  respectively, with the dotted blue lines and the dashed red lines corresponding to  $U$  and  $F$ , respectively. The plots clearly indicate that  $U$  and  $F$  are pinned to each other; that is, they move with the same velocity in spite of having different amplitudes.

$U$  and  $F$  on the  $x-t$  plane for the same choice of  $a(T)$  as before are shown in Fig. 2. Although  $a(T)$  is an arbitrary function, it should be chosen according to the situation. In the plots, we have chosen the exponential form so that the solitary wave possesses a deceleration  $-\frac{da(T)}{dT}$  that can be

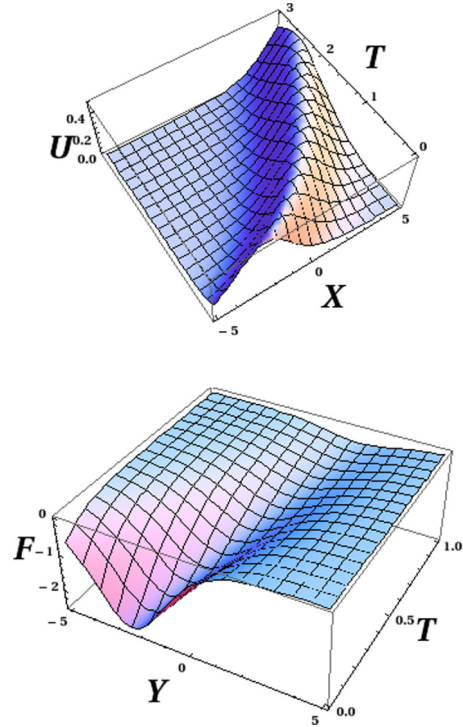


FIG. 2. Three-dimensional plots of the DIAW solution  $U$  and debris function  $F$  given by Eqs. (31) and (30), respectively, on the  $x-t$  plane for  $Y = 0$ ,  $a(T) = -5e^{-2T}$ , and  $d_1 = 1.5$ . The exponential form of  $a(T)$  causes the DIAW to decelerate with time, whereas its amplitude remains constant. On the other hand, both the amplitude and velocity of the source debris function  $F$  vary with time.

calculated from (31). Such deceleration of the solitary wave may be relevant to the real debris problem. For the periodic choice  $a(T) = 2 \cos T$ , the solitary wave solution accelerates and decelerates periodically, which is unsuitable for the debris problem. But it can be an interesting choice for other physical systems, like the shallow water wave system. If we consider the (2+1)-dimensional propagation of a free surface nonlinear shallow water wave with the periodic bottom boundary condition, then we can obtain the solitary wave solution that decelerates and accelerates periodically. The periodic bottom boundary condition means that the bottom of the channel is porous in such a way that the downward fluid velocity is a periodic function of time. Then we would get a free surface solitary wave solution with that kind of nature.

The solutions obtained so far for one solitary wave can be generalized to an  $N$  solitary wave solution  $U$  of Eq. (28) with time varying velocity. Similarly, the  $N$  debris function  $F$  that is pinned with the dust-ion acoustic solitary wave also accelerates or decelerates during propagation. Using Hirota's formalism [46,47], the two solitary wave solution  $U$  of (28) can be evaluated as

$$U = 2 [\ln G]_{XX}, \quad G = 1 + \exp(\theta_1) + \exp(\theta_2) + a_{12} \exp(\theta_1 + \theta_2), \tag{32}$$

$$a_{12} = \frac{[3k_1^2 k_2^2 (k_1 - k_2)^2 - (k_1 m_2 - k_2 m_1)^2]}{[3k_1^2 k_2^2 (k_1 + k_2)^2 - (k_1 m_2 - k_2 m_1)^2]}, \quad \theta_i = \left[ k_i X + m_i Y - \frac{k_i^4 + m_i^2}{k_i} T + \int a(T) dT \right]$$

for the choice of the debris function

$$F = 2a(T)[\ln G]_{XX}, \quad G = 1 + \exp(\theta_1) + \exp(\theta_2) + a_{12} \exp(\theta_1 + \theta_2), \tag{33}$$

$$a_{12} = \frac{[3k_1^2 k_2^2 (k_1 - k_2)^2 - (k_1 m_2 - k_2 m_1)^2]}{[3k_1^2 k_2^2 (k_1 + k_2)^2 - (k_1 m_2 - k_2 m_1)^2]}, \quad \theta_i = \left[ k_i X + m_i Y - \frac{k_i^4 + m_i^2}{k_i} T + \int a(T) dT \right],$$

where  $k_i$  and  $m_i$  are constants. Here, the amplitude of  $F$  varies with time, whereas that of  $U$  remains constant. But both  $U$  and  $F$  accelerate and decelerate with the same velocity, which depends on  $a(T)$ .

Generalizing the above solutions, the accelerated  $N$  solitary wave solution  $U$  of (28) can be obtained as

$$U = 2 [\ln G]_{XX},$$

$$G = \sum_{\mu=0,1,2} \left[ \prod_{j=1}^n \left( \frac{\beta_j}{2ik_j} \right)^{\mu_j(\mu_j-1)} (\beta_j \delta_{k_j} + \eta_j^{(0)})^{\mu_j(2-\mu_j)} \exp \left( \sum_{j=1}^n \mu_j \xi_j + \sum_{1 \leq j < l} \mu_j \mu_l A_{jl} \right) \right],$$

$$\xi_j = k_j(\omega_j T + X + \int a(T) dT + p_j Y) + \xi_j^{(0)}, \tag{34}$$

$$\eta_l = \alpha_l T + \beta_l (X + \int a(T) dT) + \gamma_l Y + \eta_l^{(0)}, \quad \gamma_j = \beta_j p_j,$$

$$\exp(A_{jl}) = \frac{(k_j - k_l)^2 - (1/3)(p_j - p_l)^2}{(k_j - k_l)^2 - (1/3)(p_j - p_l)^2}$$

for the choice of

$$F = 2 a(T) [\ln G]_{XX},$$

$$G = \sum_{\mu=0,1,2} \left[ \prod_{j=1}^n \left( \frac{\beta_j}{2ik_j} \right)^{\mu_j(\mu_j-1)} (\beta_j \delta_{k_j} + \eta_j^{(0)})^{\mu_j(2-\mu_j)} \exp \left( \sum_{j=1}^n \mu_j \xi_j + \sum_{1 \leq j < l} \mu_j \mu_l A_{jl} \right) \right],$$

$$\xi_j = k_j(\omega_j T + X + \int a(T) dT + p_j Y) + \xi_j^{(0)}, \tag{35}$$

$$\eta_l = \alpha_l T + \beta_l \left( X + \int a(T) dT \right) + \gamma_l Y + \eta_l^{(0)}, \quad \gamma_j = \beta_j p_j,$$

$$\exp(A_{jl}) = \frac{(k_j - k_l)^2 - (1/3)(p_j - p_l)^2}{(k_j - k_l)^2 - (1/3)(p_j - p_l)^2},$$

where  $k_j, \omega_j, p_j, \xi_j^{(0)}, \alpha_l, \beta_l, \gamma_l$ , and  $\eta_l^{(0)}$  are arbitrary real constants. The variation of the velocities of  $U$  and  $F$  is a result of the presence of  $a(T)$ . Thus, we have obtained a family of special exact pinned solitary wave solutions for both  $F$  and  $U$  with an accelerating and decelerating feature that may be useful in future research on this subject.

**IV. EXACT PINNED CURVED SOLITARY WAVE SOLUTION**

In the previous section, we found a family of exact pinned accelerated solitary wave solutions, the velocity of which changes over time instead of being constant. Such accelerated solitary waves move simultaneously with the charged debris object; hence, they are called pinned solitary waves. The amplitude of the dust-ion acoustic solitary wave remains constant, whereas both the amplitude and velocity of the debris function change, causing shape changing effects. Generally, in a real space plasma environment, the density localization may not always be of the form of line solitons. It may bend, twist, or turn during its propagation. Hence, to model such real physical phenomena, solitary wave solutions with arbitrary free functions that have such bending properties may be useful. Hence, along with arbitrary accelerated solitary waves, curved solitary waves on the  $x$ - $y$

plane are also important. In this section, we will try to find such exact solitary wave solutions which can bend on the  $x$ - $y$  plane depending on the forcing debris function. In [48], a numerical simulation for the propagation of a magnetosonic wave was performed with a two-dimensional circular source term. A noticeable difference from the one-dimensional (1D) simulation is observed in the shapes of wakes and precursors, which are curved in nature. This observation also strengthens the possibility of the existence of curved solitary waves in experiment. There is no generalized exact solution of the forced KP equation. In most cases, the forcing function destroys the complete integrability of the equation; hence, its exact solvability is also lost. But for certain special localized forcing functions, we can get exact solutions. An exact pinned solitary wave solution  $U$  of (28) that can bend on the  $x$ - $y$  plane is obtained in the following form:

$$U = \frac{c_1}{2} \operatorname{sech}^2 \left[ \frac{\sqrt{c_1}}{2} (X + A(Y) - c_1 T + \theta_0) \right] \tag{36}$$

for the choice of the forcing debris function  $F$  as

$$F = A_Y^2 \frac{c_1}{2} \operatorname{sech}^2 \left\{ \frac{\sqrt{c_1}}{2} [X + A(Y) - c_1 T + \theta_0] \right\} + \sqrt{c_1} A_{YY} \left( \tanh \left\{ \frac{\sqrt{c_1}}{2} [X + A(Y) - c_1 T + \theta_0] \right\} - 1 \right),$$

$X > 0$ ,

$$F = A_Y^2 \frac{c_1}{2} \operatorname{sech}^2 \left\{ \frac{\sqrt{c_1}}{2} [X + A(Y) - c_1 T + \theta_0] \right\} + \sqrt{c_1} A_{YY} \left( \tanh \left\{ \frac{\sqrt{c_1}}{2} [X + A(Y) - c_1 T + \theta_0] \right\} + 1 \right),$$

$X \leq 0$ , (37)

where  $c_1$  is a constant and  $A(Y)$  is an arbitrary function of  $Y$ . The function  $F$  in Eq. (37) vanishes as  $X \rightarrow \pm\infty$ , satisfying Poisson’s equation (4), as discussed before. There might be other choices of  $F$  to get an exact curved solitary wave solution  $U$  of (28), but we consider (37) as an example of  $F$  to explore the situation. The nonlinear function  $A(Y)$  makes the solitary wave bend in the  $x$ - $y$  plane. Both the solutions  $U$  and  $F$  given by Eqs. (36) and (37) are pinned solutions, like the solutions discussed in the previous section. As we showed in the previous section, the pinned nature can be understood by plotting both  $U$  and  $F$  with  $X$  at different times. The 3D plots of both  $U$  and  $F$  given by Eqs. (36) and (37) for a given choice of  $A(Y)$  are provided in Fig. 3. Thus, we have provided an exact pinned curved solution  $U$  for Eq. (28) for a specific choice of the localized function  $F$ . The solution may be used for modeling the twist or turn of the solitary waves during its motion in real experiments. Although there may be more general numerical or approximate solutions, the exact form of this curved solution makes it important in this field.

### V. RESULTS AND DISCUSSIONS

A few specific points of this work that need to be discussed are stated below.

(1) In this work, we have derived a few (2+1)-dimensional exact dust-ion acoustic solitary wave solutions for the choice of specific localized debris functions. The constant amplitude exact solitary waves  $U$  may accelerate or bend on the  $x$ - $t$  and  $x$ - $y$  planes, respectively, due to specific choices of the forcing functions, as discussed in Secs. III and IV.

(2) We can see that the coefficient of each term in Eq. (26) depends on  $v_p$ , which depends on  $\alpha$  via Eq. (23), i.e.,

$$v_p = \frac{1}{\sqrt{1-\alpha}}, \quad \alpha = Z_d \frac{n_{d0}}{n_{i0}}. \tag{38}$$

Hence, we can see that  $\alpha$  must be  $<1$  for a real  $v_p$ . The variation of the phase velocity  $v_p$  with parameter  $\alpha$  is plotted in Fig. 4, where we see that  $v_p$  increases with  $\alpha$ . For the ion acoustic wave, we can evaluate  $v_p$  to be equal to 1. The static dust grains increase the phase velocity by a factor of  $\frac{1}{\sqrt{1-\alpha}}$ .

(3) The solitary wave gets accelerated and decelerated due to the presence of the nonlinear function  $a(T)$ . Obviously, for  $a(T) = \text{const}$ , we get the standard line solitary waves with

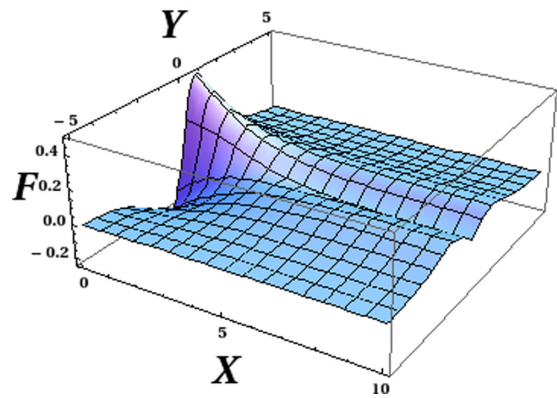
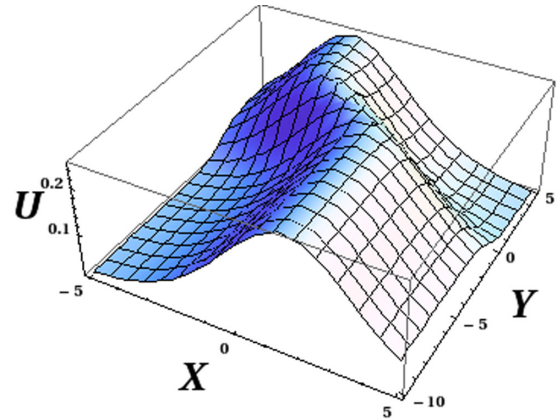


FIG. 3. Three-dimensional plots of the DIAW solution  $U$  and debris function  $F$  given by Eqs. (36) and (37), respectively, on the  $x$ - $y$  plane at  $T = 0$ ,  $c_1 = 0.5$ , and  $\theta_0 = 0$  for the choice of arbitrary function as  $A(Y) = \int \operatorname{sech} Y dY$ . It can be easily seen that both  $U$  and  $F$  get curved on the  $x$ - $y$  plane.

constant velocity. The acceleration of the solitary wave is shown by the contour plots in Figs. 5 and 6.

(4) The exact accelerated solitary wave solution (31) can be expressed in old variables as:  $\xi, \eta$  and  $\tau$  (used during

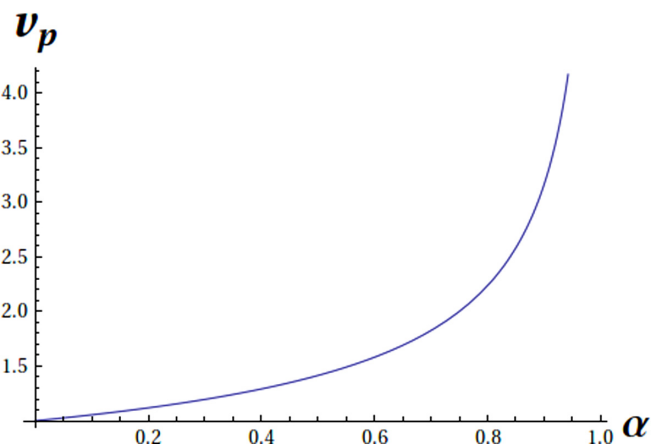


FIG. 4. Variation of phase velocity  $v_p$  with  $\alpha$ .

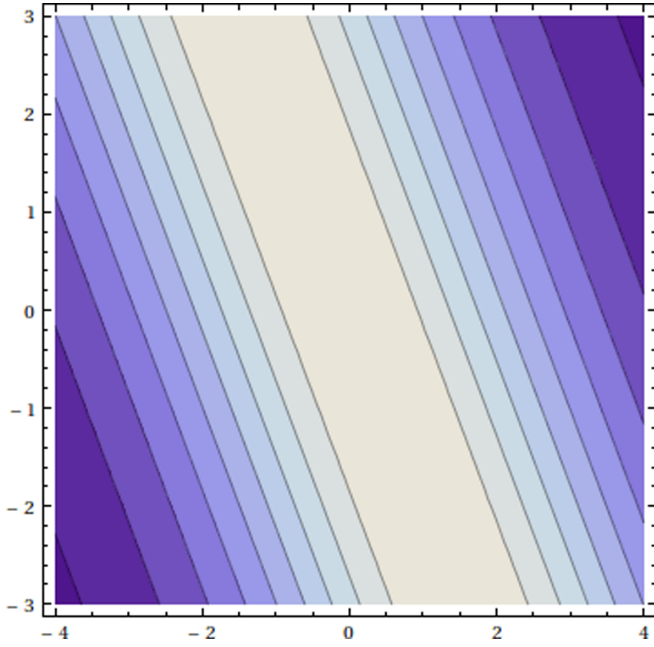


FIG. 5. The contour plot of the DIAW solution  $U$  (31) in the  $x-t$  plane for  $Y = 0$ ,  $a(T) = 2$ ,  $d_1 = 1.5$ . We can see that the peak of the solitary wave  $U$  moves along a straight line in the  $x-t$  plane for  $a(T) = \text{const}$ , thus showing the usual line solitary waves.

derivation of forced KP equation in the manuscript)

$$n_1 = \frac{3B(d_1 - 1)}{A} \operatorname{sech}^2 \left[ \frac{\sqrt{d_1 - 1}}{2} \left\{ \xi + \sqrt{(B/C)\eta} - d_1 B \tau \right. \right. \\ \left. \left. - \left( \frac{60B^3}{DA} \right) \int \exp(-2B\tau) d\tau \right\} \right], \quad (39)$$

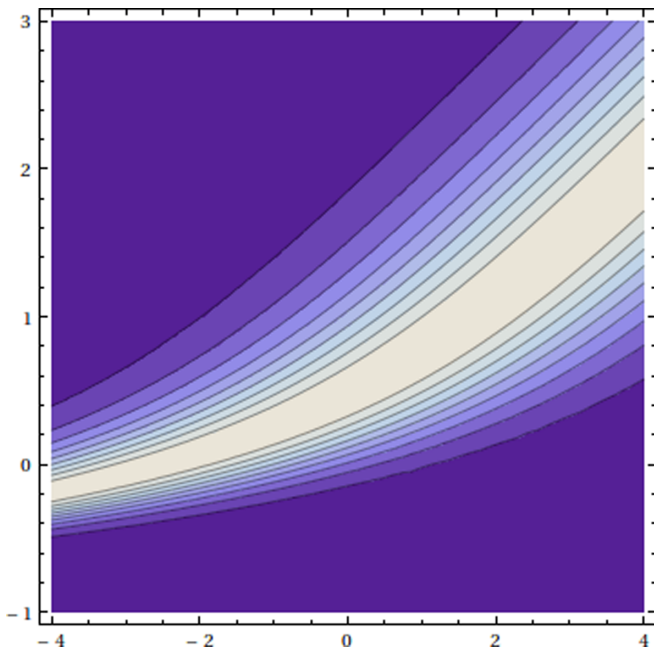


FIG. 6. The contour plot of the DIAW solution  $U$  (31) in the  $x-t$  plane for  $Y = 0$ ,  $a(T) = -5e^{-2T}$ ,  $d_1 = 2$ . We can see that the peak of the solitary wave  $U$  moves along a curved path in the  $x-t$  plane for the exponential form of  $a(T)$ .

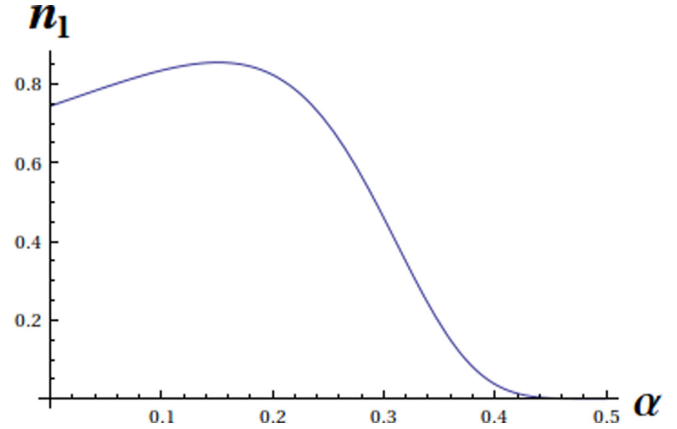


FIG. 7. The variation of the DIAW  $n_1$  in (39) with  $\alpha$  at the center  $\xi = \eta = 0$  at  $\tau = 1$  for  $d_1 = 1.5$ .

where the coefficients  $A$ ,  $B$ , and  $C$  are given as

$$A = \frac{v_p(3 - v_p^2)}{2}, \quad B = \frac{v_p^3}{2}, \quad C = D = \frac{v_p}{2} \quad (40)$$

for  $a(T) = -5e^{-2T}$ . The variation of the DIAW  $n_1$  in (39) with  $\alpha$  at the center  $\xi = \eta = 0$  at  $\tau = 1$  is shown in Fig. 7.

(5) In this work, we have also derived an exact curved solitary wave solution for a special localized debris function. The exact solitary wave solution can bend on the  $x-y$  plane depending on the forcing function. In [48], a two-dimensional circular source term was considered in their numerical simulation for the propagation of a magnetosonic wave. The noticeable difference from the 1D simulation is in the shapes of wakes and precursors, which are curved in nature. This observation also strengthens the possibility of observing the exact curved solitary wave solution (36) in the experimental scenario. It should be noted that the curvature of the solution (36) occurs due to the presence of the nonlinear function  $A(Y)$  in the argument of the solution (36). Now it is necessary to determine how much curvature takes place by varying  $A(Y)$ , i.e., what the condition is for larger bending. For the static case ( $T = 0$ ), the locus of the maximum amplitude of the curved solitary wave solution (36) is of the form

$$\frac{\sqrt{c_1}}{2} [X + A(Y) + \theta_0] = 0. \quad (41)$$

Now taking the derivative with respect to  $Y$  twice in Eq. (41) we get

$$\frac{dS}{dY} = -A_{YY}, \quad (42)$$

where the slope is defined as  $S = \frac{dX}{dY}$ . We see from (42) that for a higher value of right-hand side, the rate of variation of the slope  $S$  will be higher. Hence, in that case, the slope of the maximum amplitude curve will vary large for traversing the unit distance in  $Y$ . Larger rate of variation of slope  $S$  describes larger bending. Hence, for large bending of solitary waves to take place, the double derivative of  $A(Y)$  must also be high. This is explained clearly by the contour plot in Fig. 8.

(6) Similar to the exact solutions obtained in [7], we derive a few intricate exact solitary wave solutions. The only difference is the solutions derived in [7] are line solitary



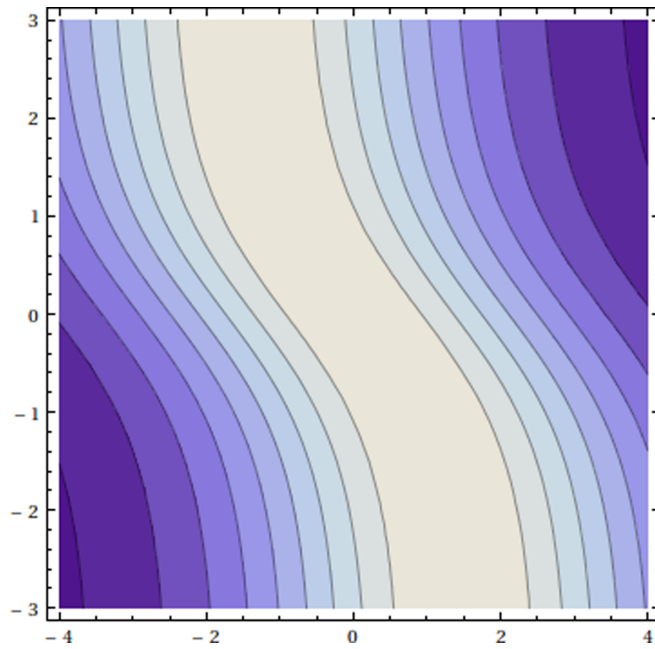


FIG. 8. Contour plot of the curved dust-ion acoustic solitary wave solution  $U$  given by Eq. (36) on the  $x$ - $y$  plane at  $T = 0$  for  $c_1 = 0.5$ ,  $\theta_0 = 0$ , and  $A(Y) = \int \text{sech}Y dY$ . The plot shows that the DIAW solution  $U$  bends on the  $x$ - $y$  plane due to the function  $A(Y)$ .

waves, whereas the solutions derived in the present work are accelerated and curved solitary waves. Basically, we have investigated a few specific forms of  $F$  for which we get exact solitary wave solutions for  $U$  with bending features. The velocity profiles for both  $U$  and  $F$  are found to be identical. For other general choices of  $F$ , perturbative or numerical solutions need to be obtained.

## VI. CONCLUDING REMARKS

In this work, we have considered the low temperature and low density plasma in the LEO region in the presence of localized charged space debris particles. The dynamics of (2+1)-dimensional nonlinear dust-ion acoustic waves induced in the system is found to be governed by the forced KP-II equation, where the forcing term depends on the charged space debris function. We have found some exact curved solitary wave solutions for the DIAW that can bend on the  $x$ - $t$  and  $x$ - $y$  planes. A family of exact pinned accelerated solitary wave solutions (30)–(35) has been derived. The velocity of the solutions changes over time, whereas the amplitude remains constant. The solutions contain an arbitrary time dependent function  $a(T)$  that can be chosen accordingly for modeling different types of dynamics of the solutions. Also, a special exact solitary wave solution (36) has been derived for a special debris function (37) that gets curved on the  $x$ - $y$  plane, where its curvature depends on the nature of the forcing debris function. The solution also contains an arbitrary function  $A(Y)$ . For different choices of  $A(Y)$ , we would get different kinds of bending of the solitary wave. Thus, the exact solutions of this work may be interesting to the nonlinear dynamics community and useful for different practical applications.

## ACKNOWLEDGMENTS

S.P.A. acknowledges the Department of Atomic Energy (DAE) of the government of India for financial help during this work through the institute fellowship scheme. A.M. would like to acknowledge the Indian Statistical Institute, Kolkata, for the financial support during this research work, and is indebted to K. Kar for discussions during the progress of the work. The authors are grateful to the anonymous reviewers for their fruitful suggestions to improve this work.

- [1] National Research Council, *Space Plasma Physics: The Study of Solar-System Plasmas* (National Academies Press, Washington, DC, 1978).
- [2] H. Klinkrad, *Space Debris Models and Risk Analysis*, Springer Praxis Books (Praxis Publishing, Chichester, UK, 2006).
- [3] J. C. Sampaio, E. Wnuk, R. Vilhena de Moraes, and S. S. Fernandes, Resonant orbital Dynamics in LEO region: Space debris in focus, *Math. Probl. Eng.* **2014**, 929810 (2014).
- [4] I. Kulikov and M. Zak, Detection of moving targets using soliton resonance effect, *Adv. Remote Sens.* **1**, 58 (2012).
- [5] M. Horányi, Charged dust dynamics in the solar system, *Annu. Rev. Astron. Astrophys.* **34**, 383 (1996).
- [6] United Nations, *Technical Report on Space Debris* (United Nations, New York, 1999).
- [7] A. Sen, S. Tiwari, S. Mishra and P. Kaw, Nonlinear wave excitations by orbiting charged space debris objects, *Adv. Space Res.* **56**, 429 (2015).
- [8] S. P. Acharya, A. Mukherjee, and M. S. Janaki, Accelerated magnetosonic lump wave solutions by orbiting charged space debris, *Nonlinear Dyn.* **105**, 671 (2021).
- [9] S. K. Tiwari and A. Sen, Wakes and precursor soliton excitations by a moving charged object in a plasma, *Phys. Plasmas* **23**, 022301 (2016).
- [10] S. K. Tiwari and A. Sen, Fore-wake excitations from moving charged objects in a complex plasma, *Phys. Plasmas* **23**, 100705 (2016).
- [11] S. Jaiswal, P. Bandyopadhyay, and A. Sen, Experimental observation of precursor solitons in a flowing complex plasma, *Phys. Rev. E* **93**, 041201(R) (2016).
- [12] G. Arora, P. Bandyopadhyay, M. G. Hariprasad, and A. Sen, Effect of size and shape of a moving charged object on the propagation characteristics of precursor solitons, *Phys. Plasmas* **26**, 093701 (2019).
- [13] P. K. Shukla and V. P. Silint, Dust ion-acoustic wave, *Phys. Scr.* **45**, 508 (1992).
- [14] P. K. Shukla and A. A. Mamun, Introduction to dusty plasma physics, *Plasma Phys. Control. Fusion* **44**, 395 (2002).
- [15] S. S. Duha, M. G. M. Anowar, and A. A. Mamun, Dust ion-acoustic solitary and shock waves due to dust charge fluctuation with vortexlike electrons, *Phys. Plasmas* **17**, 103711 (2010).

- [16] A. A. Mamun and S. Islam, Nonplanar dust-ion-acoustic double layers in a dusty nonthermal plasma, *J. Geophys. Res.* **116**, A12323 (2011).
- [17] S. I. Popel and M. Y. Yu, Ion acoustic solitons in impurity-containing plasmas, *Contrib. Plasma Phys.* **35**, 103 (1995).
- [18] G. C. Das, J. Sarma, and R. Roychoudhury, Some aspects of shock-like nonlinear acoustic waves in magnetized dusty plasma, *Phys. Plasmas* **8**, 74 (2001).
- [19] M. G. M Anwar and A. A. Mamun, Multidimensional instability of dust-ion-acoustic solitary waves, *IEEE Trans. Plasma Sci.* **36**, 2867 (2008).
- [20] A. A. Mamun, R. A. Cairns, and P. K. Shukla, Dust negative ion acoustic shock waves in a dusty multi-ion plasma, *Phys. Lett. A* **373**, 2355 (2009).
- [21] R. L. Merlino and J. A. Goree, Dusty plasmas in the laboratory, industry, and space, *Phys. Today* **57**(7), 32 (2004).
- [22] O. Rahman and A. A. Mamun, Dust-ion-acoustic solitary waves in dusty plasma with arbitrarily charged dust and vortex-like electron distribution, *Phys. Plasmas* **18**, 083703 (2011).
- [23] S. Yasmin, M. Asaduzzaman, and A. A. Mamun, Evolution of higher order nonlinear equation for the dust ion-acoustic waves in nonextensive plasma, *Phys. Plasmas* **19**, 103703 (2012).
- [24] F. Verheest, T. Cattaert, and M. A. Hellberg, Ion- and dust-acoustic solitons in dusty plasmas: Existence conditions for positive and negative potential solutions, *Phys. Plasmas* **12**, 082308 (2005).
- [25] A. A. Mamun, P. K. Shukla, and B. Eliasson, Solitary waves and double layers in a dusty electronegative plasma, *Phys. Rev. E* **80**, 046406 (2009).
- [26] F. Verheest, M. A. Hellberg, and I. Kourakis, Dust-ion-acoustic supersolitons in dusty plasmas with nonthermal electrons, *Phys. Rev. E* **87**, 043107 (2013).
- [27] A. A. Mamun and P. K. Shukla, Cylindrical and spherical dust ion-acoustic solitary waves, *Phys. Plasmas* **9**, 1468 (2002).
- [28] A. A. Mamun, Effects of adiabaticity of electrons and ions on dust-ion-acoustic solitary waves, *Phys. Lett. A* **372**, 1490 (2008).
- [29] A. A. Mamun, and P. K. Shukla, Effects of nonthermal distribution of electrons and polarity of net dust-charge number density on nonplanar dust-ion-acoustic solitary waves, *Phys. Rev. E* **80**, 037401 (2009).
- [30] R. Bharuthram and P. K. Shukla, Large amplitude ion-acoustic solitons in a dusty plasma, *Planet. Space Sci.* **40**, 973 (1992).
- [31] A. S. Truitt and C. M. Hartzell, Simulating plasma solitons from orbital debris using the forced Korteweg-de Vries equation, *J. Spacecr. Rockets* **57**, 5 (2020).
- [32] A. S. Truitt and C. M. Hartzell, Three-dimensional Kadomtsev-Petviashvili damped forced ion acoustic solitary waves from orbital debris, *J. Spacecr. Rockets* **58**, 3 (2021).
- [33] A. Mukherjee, S. P. Acharya, and M. S. Janaki, Dynamical study of nonlinear ion acoustic waves in presence of charged space debris at low Earth orbital (LEO) plasma region, *Astrophys. Space Sci.* **366**, 7 (2021).
- [34] A. S. Truitt and C. M. Hartzell, Simulating damped ion acoustic solitary waves from orbital debris, *J. Spacecr. Rockets* **57**, 5 (2020).
- [35] R. Ali, A. Saha, and P. Chatterjee, Analytical electron acoustic solitary wave solution for the forced KdV equation in superthermal plasmas, *Phys. Plasmas* **24**, 122106 (2017).
- [36] P. Chatterjee, R. Ali, and A. Saha, Analytical solitary wave solution of the dust ion acoustic waves for the damped forced Korteweg-de Vries equation in superthermal plasmas, *Z. Naturforsch. A* **73**, 151 (2018).
- [37] H. Zhen, B. Tian, H. Zhong, W. Sun, and M. Li, Dynamics of the Zakharov-Kuznetsov-Burgers equations in dusty plasmas, *Phys. Plasmas* **20**, 082311 (2013).
- [38] L. Mandi, A. Saha, and P. Chatterjee, Dynamics of ion-acoustic waves in Thomas-Fermi plasmas with source term, *Adv. Space Res.* **64**, 427 (2019).
- [39] A. N. Dev, J. Sarma, M. K. Deka, A. P. Misra, and N. C. Adhikar, Kadomtsev-Petviashvili (KP) Burgers equation in dusty negative ion plasmas: Evolution of dust-ion acoustic shocks, *Commun. Theor. Phys.* **62**, 875 (2014).
- [40] H. U. Rehman, Kadomtsev-Petviashvili equation for dust ion-acoustic solitons in pair-ion plasmas, *Chin. Phys. B* **22**, 035202 (2013).
- [41] O. Rahman and Md. M. Haider, Modified Korteweg-de Vries (mK-dV) equation describing dust-ion-acoustic solitary waves in an unmagnetized dusty plasma with trapped negative ions, *Adv. Astrophys.* **1**, 161 (2016).
- [42] R. Grimshaw, M. Maleewong, and J. Asavanant, Stability of gravity-capillary waves generated by a moving pressure disturbance in water of finite depth, *Phys. Fluids* **21**, 082101 (2009).
- [43] R. A. Kraenkel, J. G. Pereira, and M. A. Manna, The reductive perturbation method and the Korteweg-de Vries hierarchy, *Acta Appl. Math.* **39**, 389 (1995).
- [44] A. Kundu, Exact accelerating solitons in nonholonomic deformation of the KdV equation with a two-fold integrable hierarchy, *J. Phys. A* **41**, 495201 (2008).
- [45] A. Kundu, Nonholonomic deformation of KdV and mKdV equations and their symmetries, hierarchies and integrability, *J. Phys. A* **42**, 115213 (2009).
- [46] A. M. Wazwaz, Multiple-soliton solutions for the KP equation by Hirota's bilinear method and by the tanh-coth method, *Appl. Math. Comput.* **190**, 633 (2007).
- [47] A. Mukherjee, M. S. Janaki, and A. Kundu, Bending of solitons in weak and slowly varying inhomogeneous plasma, *Phys. Plasmas* **22**, 122114 (2015).
- [48] A. Kumar and A. Sen, Precursor magneto-sonic solitons in a plasma from a moving charge bunch, *New J. Phys.* **22**, 073057 (2020).